Date of Publication: 14th May 2026
ISSN: 2737-713X

THE MANUFACTURE AND MORPHOLOGICAL CHARACTERIZATION OF NNSUPA NON-CHEMICAL CERAMIC FILTER CANDLE IN THE PURIFICATION OF WATER IN GHANA

*[1]Michael Commeh, [2]James Hawkins Ephraim, [3]Kwabena Bonsu Kusi, [4]David Dodoo-Arhin

[1] *Technology Consultancy Centre, College of Engineering, Kwame Nkrumah University of Science and Technology, KNUST - Kumasi, Ghana*
[2] *Comeph & Associates Ghana. Ltd., Oyarifa, Accra, Ghana*
[3] *Smart Aid Consult, Kumasi Innovation Hub, KNUST - Kumasi, Ghana*
[4] *Department of Materials Science and Engineering, University of Ghana, P. O. Box LG 77, Legon-Accra, Ghana*
***Corresponding author:** mcommeh.tcc@knust.edu.gh*

Abstract

Ceramic household water filters have been identified as a simple and scalable water treatment technology to help meet the world's growing demand for potable and affordable drinking water. However, the high cost and potentially toxic nature of colloidal silver, which is mostly used in filter manufacturing, have made it essential to develop affordable and safer ceramic filters. This study fabricated and investigated the morphological characteristics of the Nnsupa ceramic filter for water treatment. Locally sourced clays mixed with starch were moulded, dried, and fired to produce filters called NHCWF filters. The structural properties, microscopic characteristics, and physicochemical parameters of the filters were then characterised. Scanning Electron Microscopy showed a closely packed ceramic structure with scattered porosity. The filters showed multilayer adsorption with a type IV isotherm during gas physisorption analysis, which, combined with mercury intrusion porosimetry, demonstrated the presence of micropores, mesopores, and macropores. The pore sizes of the filters ranged from 0.01 to 10.0 µm, with log reduction values ranging between 4 (99.99%) and 5 (99.999%), which meet both Ghanaian and WHO drinking water standards. Fourier transform infrared analysis also indicated the presence of functional groups consumed over time when the filters were used. The average flow rate of filtered water under gravity was 0.27 L h^{-1} with an experimental filtering setup that used the NHCWF filter. This study has shown that the NHCWF presents as a feasible alternative to conventional silver-embedded ceramic filters used in household production of potable drinking water.

Keywords
Ceramic water filtering, non-chemical filter, sustainable water treatment, low-cost water treatment, innovative filtering

Introduction

According to the United Nations, Sustainable Development Goal (SDG) 6 is to "ensure availability and sustainable management of water and sanitation for all" (United Nations, 2023). Among the targets of this goal is "to achieve universal and equitable access to safe and affordable drinking water for all" by 2030. To meet this target, an increase in the supply of safely managed drinking water by approximately 763,000 people daily for the next 8 years is required (in D. Team and Roser, 2023; United Nations, 2023). However, this goal of providing safely managed drinking water for all remains a challenge. This issue is especially severe in low- and middle-income countries with inadequate infrastructure and prevalent water contamination. Traditional water treatment methods, including chlorination and UV treatment, often fail to reach underserved populations due to their reliance on electricity, complex infrastructure, and high operational costs (Null et al., 2018). Ghana, for example, has established multiple water treatment plants and supply projects which have contributed to improving access to drinking water and the health of its citizenry. Currently, waterborne diseases caused by helminths are no longer prevalent in Ghana (Aakumiah, 2007). However, about 56% of Ghanaians do not have access to safely managed drinking water and basic drinking water services, respectively (in D. Team and Roser, 2023). Again, the country still has communities that suffer the effects of contaminated water due to the lack of access to potable water sources. The most common diarrheal diseases in Ghana are giardiasis and cholera, which are mostly attributed to the consumption of contaminated water (Kakulu, 2012).

Ceramic water filters (CWFs) have emerged as a viable water treatment alternative due to their low cost, ease of use, and ability to remove bacteria, protozoa, and other contaminants (Yang et al., 2020). However, most ceramic filters currently rely on silver nanoparticles as a biocide, posing environmental and health risks due to silver leaching into the water supply and the development of microbial resistance.

The use of silver nanoparticles in ceramic filters has raised environmental and health concerns, including the potential for toxicity to aquatic life and the development of silver-resistant bacterial strains. Research by Benn et al. (2010) has demonstrated that silver nanoparticles can leach into the environment during the use of these filters, potentially contaminating water sources and harming ecosystems. Also, the WHO has expressed concerns about the long-term health effects of chronic exposure to silver in humans, which has been shown to potentially result in conditions such as argyria (permanent skin discolouration) or even DNA damage (Venis and Basu, 2021; Wadhera and Fung, 2005). Research has shown the possibility of elution of an average silver quantity range of 0.02–1.4 mg for each litre of filtrate produced by silver-based CWF (Ehdaie et al., 2017; Lyon-Marion et al., 2018; Mikelonis et al., 2016;

Mittelman et al., 2015; Nunnelley et al., 2016; Oyanedel-Craver and Smith, 2008; Ren and Smith, 2013). Hence, using it may result in the silver concentration of effluent exceeding the WHO's recommended limit of 0.1 mg L^{-1}. Furthermore, the reliance on silver in water filtration technologies presents a significant barrier to achieving this SDG goal 6 due to the environmental and economic costs associated with silver mining, production, and disposal (Medici et al., 2019). The development of non-silver-based ceramic filters can contribute to a more sustainable approach to water treatment by reducing the environmental impact of water purification processes and supporting the transition to greener technologies. Moreover, non-silver-based filters could be more cost-effective in the long term, as they avoid the escalating costs and resource limitations associated with silver production. This aligns with the broader objectives of SDG 12 (Responsible Consumption and Production), which calls for the reduction of hazardous substances in products and processes (United Nations, 2023). Consequently, there is a pressing need to develop non-silver-based CWF alternatives that are equally or more effective in eliminating waterborne pathogens without the associated risks. Investing in research and development, particularly focusing on the development of new materials and the refinement of manufacturing processes, not only addresses an immediate public health need but also supports global efforts toward sustainability and environmental stewardship. Promising innovations include the use of plant-based biocides, metal oxide nanoparticles, and functionalised ceramic materials that exhibit strong antimicrobial properties without the associated risks of silver. These alternatives have shown potential in preliminary studies, but further research is required to optimise their effectiveness, durability, and cost-efficiency.

This study was aimed at fabricating and characterising a non-silver-based CWF that meets the WHO drinking water treatment standards using naturally functionalised ceramic materials that are readily available and easily sourced.

Materials and Methods

The raw materials used in this project were sourced from Ghana. Kaolin clay was sourced from the Telekou Bokasso near Nkroful, Western Region to Ekon east of Cape Coast market, and Mfensi plastic clay from Mfensi, a small town in the Ashanti Region. Cassava starch was also sourced from the Ayigya market in the Ashanti Region.

Fabrication Process

The raw materials including Kaolin clay, Mfensi plastic clay, and gelatinised cassava starch were mixed in a ratio of 10:1.5:1 by weight respectively. Thirteen Kilograms (13 kg) of water was added to the mixture. The mixture was suspended in water by adding 0.45 g (5% of the total weight of the composition) of "formil AP" electrolyte. Formil AP (sodium Silicate (Na_2SO_4)) is affordable and readily available on the Ghanaian market. The mixture was then blunged into a slurry at 2600 rpm for one hour using a Black and Decker Insulated Super Power Driver 3/3 inches (10 mm) drill (220 V, 1.7 A, 370 W, 2600 rpm).

After stirring, the entire slurry was sieved through an 80 mesh sieve (0.007 inches or 0.18 mm width of the opening of the sieve) and poured into 50 dried plaster of Paris (POP) moulds. The slurry was left in the POP moulds for about 30 sec to allow for water to be sucked from the mixture. When the setup was half-dried, the work-in-progress ceramic filter moulds were removed by turning the POP mould upside down, and the filters detached from the POP Mould.

The released filters were dried in a natural indoor environment and fired in an old manually operated gas kiln in an oxidation atmosphere equivalent to that of Tru-Fire gas kiln, D.J. Webb-Bednall, Stafford, using a nickel-chrome thermocouple with a GMH 3219 Digital thermometer manufactured by Greisinger Electronic as a temperature measuring tool. The firing was done over 12 hours with the temperature increasing slowly at a rate ranging between 1.0 °C min^{-1} and 2.5 °C min^{-1} till it reached 1050 °C.

After firing, the filter candle is cooled with natural air and fitted with a plastic holder at its opened end. Appendix A shows a schematic representation of the experimental design setup.

Determination of Physicochemical and Microstructural Properties of Filter Candles

A sample of the filter candles was randomly selected for a particle size distribution experiment before the firing process. The experiment was conducted at the Civil Engineering Department of the Kwame Nkrumah University of Science and Technology (KNUST) using the sieve method as shown in Appendix B.

Three samples of the fired filter candles were randomly selected from the ceramic filter candles produced and analysed for microstructural and physicochemical properties. Experiments were conducted at the Regional Water and Environmental Sanitation Centre Kumasi (RWESCK) of KNUST on the samples selected for pore distribution and characterisation of the filter candle including mercury intrusion porosimetry experiment (Zeng et al., 2020), nitrogen gas physisorption experiment (Micromeritics, 2013; Thommes et al., 2015), and scanning electron microscopy (SEM) experiment.

Nitrogen adsorption–desorption isotherms were obtained at 77 K using N_2 as the adsorptive. Before the analysis, samples were degassed at 105 °C for 2 h to remove adsorbed moisture. Specific surface area was determined using the Brunauer–Emmett–Teller (BET) method. Mesopore size distributions were calculated using the Barrett–Joyner–Halenda (BJH) model applied to the desorption branch. Micropore analysis was conducted using the t-plot method.

Microstructural characterization was performed using scanning electron microscopy (SEM). Images were acquired at magnifications ranging from 50× to 5000×, corresponding to millimetre- and micrometre-scale observations. SEM operating conditions were as follows: accelerating voltage of 10

kV, working distance of 10 mm, and detector type secondary electron detector.

In addition to a sample of the new filters produced, a 14-month-used filter produced using the same method as employed in this study was analysed for the identification of functional groups. Fourier transform infrared (FTIR) experiment (Solomon and Carangelo, 1982; Zagonel et al., 2004) was conducted at RWESCK, KNUST to investigate the presence of functional groups in the filter candles.

Experimental Setup for Flow Rate Determination and Bacteria Retention Analysis

An experimental setup composed of a 15-litre bucket (receiver) with a 2.5 cm hole in the middle of its base, a 40-litre container (dispenser) that empties through a tap fitted at its lower exterior, and a collector. A sample of the NHCWF was fitted in the receiver to form a tight impermeable joint. The receiver was then installed in the opening of the dispenser and sealed with a nontoxic adhesive. About 1 L of clean hot water was poured into the receiver to percolate through the filter and clean the system. After the system cleansing was complete, the setup was drained and left to dry for approximately 12 hrs. The collector was installed underneath the tap for discard collection, and the setup was ready to use. Appendix D shows a schematic representation of the experimental design setup.

Filtration Rate Determination

About 5 L of water sourced from the Wiwi river was poured into the receiver and allowed to percolate through the filter candle into the dispenser. After every 10-minute interval since the first drop, the content of the dispenser was emptied into the collector, and the volume of the water was measured and recorded as $v_{\#}$. The collector was then discarded, and the process was repeated without replacing or topping up the water in the receiver. A total of 13 trials of the experiment were conducted. Data collected during the wet-up phase (the initial saturation of the ceramic matrix), corresponding to the 10 mins of the experiment, was excluded from filtration rate analysis. Steady-state conditions were assumed once the highest average flow rate was recorded.

The data that fell within the steady-state conditions were then used to calculate the filtration rate of the NHCWF filter with the equation:

$$\text{Flow Rate (V)} = \frac{V_1 + V_2 + V_3 + \cdots\cdots\cdots + V_{12} + V_{13}}{130} \quad (1)$$

Determination of Bacteria Retention Ability of Filter Candles

The bacteria retention ability of the filters was determined by investigating the microbial concentration of the industrial wastewater sample before and after a filtration process with the experimental setup. Four different setups were mounted as shown in Appendix D, each fitted with a randomly selected sample from the ceramic filters produced with three of the receivers filled with water sourced from the Wiwi River (feed water), and the fourth filled with an influent blank (sterile) water sample. Each setup filled with water sampled from the Wiwi River was served a single trial of the experiment, and the setup with sterile water served as the control. About 1 L of the feed water and 1 L of percolate water samples from each setup were simultaneously collected into sterile sampling bottles. The water samples were immediately conveyed to the lab in a cooler with ice packs for multiple bacterial retention experiments.

The bacterial retention ability (log reduction values) of the filter candles was investigated using the pour plate method and photometric experiments (optical density (OD) experiment (Campbell, 2010; Meyers et al., 2018) and ATP bioluminescence experiment (Deininger and Lee, 2001)). These techniques were used to quantify the concentration of *Escherichia coli* and *Bacillus subtilis* contained in the feed and permeate water samples.

Prior to the sample analysis, method detection limits (MDLs) were established for all the analytical procedures used. For the pour plating method, the MDL was defined as the minimum detectable colony-forming units (CFU) per unit volume. On the other hand, the lowest measurable relative light unit (RLU) distinguishable from background noise was used for the photometric experiments.

The results were evaluated to determine the bacteria retention efficiency of the NHCWF by calculating the log reduction value (LRV), depending on the bacteria concentration recorded in the feed water sample (C_f) and the permeate water sample (C_p). LRV was calculated for each trial with the equation:

$$\text{LRV} = \log_{10}\left(\frac{C_f}{C_p}\right) \quad (2)$$

For these calculations, censored data were treated using threshold-based substitution (i.e., assuming counts at the detection limit). The results were averaged across replicates and reported as mean ± standard deviation (SD) with the equations:

$$\text{Mean}(\bar{x}) = \frac{x_1 + x_2 + x_3}{3} \quad (3)$$

$$\text{Standard Deviation}(s) = \sqrt{\frac{\sum (x_i - \bar{x})^2}{n-1}} \quad (4)$$

Results and Discussions

Results

The Nnsupa Household Ceramic Water Filter (NHCWF)

The fabricated filter candle was dubbed the Nnsupa household ceramic water filter (NHCWF). It was composed of a U-shaped semi-rough-textured clay-based candle that sits on a plastic holder, as shown in Figure 1a. The average height

Table 1. Per-Unit Production Cost Breakdown as of the year 2021 in USD ($)

Component	Cost (per batch) / $	Units per batch	Cost per unit / $
Raw materials	880.00	1000	0.88
Energy (kWh)	90.00	1000	0.09
Labour and Equipment Cost	400.00	1000	0.40
Total	—	—	**$1.37**

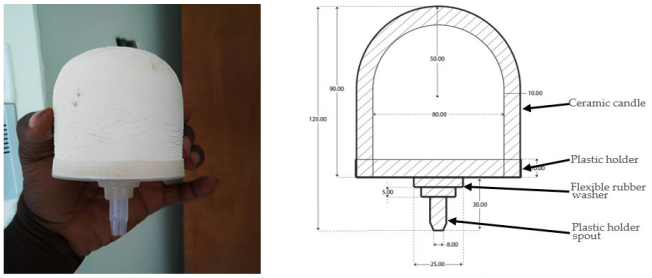

(a) (b)

Figure 1. (a) A picture of the NHCWF filter; (b) A labelled Schematic Cross-Sectional Drawing of the NHCWF filter with dimensions in mm

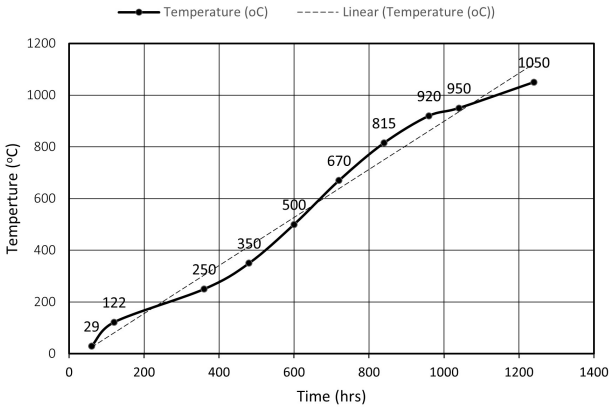

Figure 2. Firing regimen for a batch (1000 units) of the NHCWF filter candles

of the complete filter set is 12 cm. Its clay-based candle has an average inner opening diameter of 8 cm, an average outer diameter of 10 cm, and an average height of 9 cm. The opening of the clay-based candle sits in the plastic holder such that the rim of the plastic holder flanks and flushes with a 1 cm periphery of the opened end of the candle. This forms a tight joint that remains nonporous to water. The 4 cm tall plastic holder has a 0.8 cm spout and a 2.5 cm wide rubber washer. A cross-sectional diagram of the complete filter set is shown in Figure 1b.

Cost Analysis

The cost analysis of the NHCWF filter candle focused on key factors such as raw material costs, energy consumption during production, labour, and equipment expenses.

The primary materials used in the fabrication of the ceramic filter candle include Kaolin clay used to enhance the mechanical strength of the filter, Mfensi plastic clay, a proprietary additive to enhance porosity, and cassava starch to serve as pore-forming material. For each filter produced, the cost of each material is $0.33, $0.17, and $0.09, respectively, resulting in a total raw material cost of $0.67. An additional cost for packaging, including the cost of the plastic holder and glue for installation, amounts to $0.21.

Energy consumption is primarily driven by the sintering process, where the ceramic material is heated to high temperatures. The NHCWF filter requires a sintering temperature of 1050 °C, which is produced using LPG gas. The firing regimen is as shown in Figure 2.

The energy cost was calculated with the following equation:

$$\text{Energy cost per filter} = \frac{\text{Total energy consumption (Kg)}}{\text{number of filters per batch}} \times \text{gas cost (per Kg)} \quad (5)$$

Labour and equipment costs were estimated based on the resources required for each production stage, including moulding, drying, and sintering. Despite its refined fabrication process, the NHCWF filter has a fast production rate. A labourer can weigh, mix, sieve, and cast about 100 ceramic candles in less than 2 hours. Sintering also generally takes less than 2 hours to complete. The labour and equipment (Plaster of Paris mould used for casting) costs incurred per unit filter produced are $0.20 and $0.20, respectively.

The per-unit cost of the NHCWF filter is presented in Table 1.

The Particle Size Distribution of NHCWF Materials

Three categories of particles; clay (particle sizes below 0.002 mm), silt (particle sizes ranging between 0.002 and 0.6 mm), and sand (particle sizes between 0.6 and 2.0 mm) were identified in a particle size distribution experiment conducted on the NHCWF candles. Appendix C shows a graphical depiction of the particle size distribution of the unfired filter candle. The results indicated that silt makes up the bulk of the total particles within the filter candle as shown in Table 2 (78% by weight of total composition).

Scanning Electron Microscopy (SEM) Results

Figure 3 shows pictures of the NHCWF filter candle and its SEM micrograph labelled A, B, C, and D. At 5 cm resolution, Figure 3A shows a complete filter candle with its holder installed and ready for use in a ceramic water filtering setup, whilst Figure 3B shows the inner parts of the filter candle. Figure 3C and Figure 3D also show an SEM micrograph of

Table 2. Particle size distribution of NHCWF Filter Candle

Particle	Sizes (mm)	Composition (% by weight)
Clay	<0.002	9
Silt	0.002–0.6	78
Fine/medium/coarse sand	0.6–2.0	13

Table 3. Particle characteristics of Nnsupa Ceramic Filter Candle

Analytical method	Parameter	Units	Sample 1	Sample 2	Sample 3
Hg-porosimetry	Pore diameter range	µm	2–10	1–10	2–10
	d_{50}	µm	6.9	6.3	8.5
	Open Porosity	%	49.4	48.1	53.8

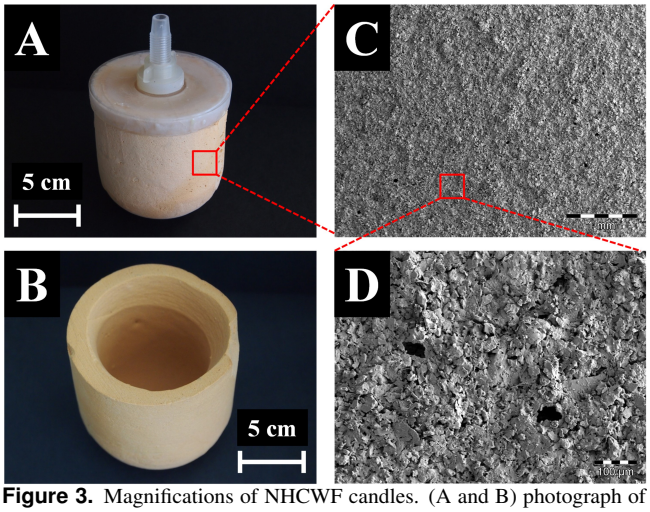

Figure 3. Magnifications of NHCWF candles. (A and B) photograph of the filter crucible with cover plate and presentation of the inner filter part, respectively, (C and D) SEM micrographs of the filter structure (overview in the mm-scale and detailed view in the µm-scale, respectively)

the morphology of a fragment of the Nnsupa ceramic filter candle at different resolutions. They show a 1 mm and 100 μm resolution of the filter candle respectively. At these resolutions, the microstructure of the filter candles is observed as being rough in texture. The micrographs show the presence of microscopic pores in the filter candle. As shown in Figure 3C and even more visible in the higher resolutions of Figure 3D, the pores are revealed as dark-coloured spots or areas cemented in between the clay matrix, also shown in grey colours.

Mercury Intrusion Porosimetry (MIP) Results

From the results of the mercury intrusion porosimetry (MIP) experiment, the pore diameters of filter samples 1, 2, and 3 were recorded as ranging from 2–10 μm (d_{50} = 6.9 μm), 1–10 μm (d_{50} = 6.3 μm), and 2–10 μm (d_{50} = 8.5 μm) respectively. The open porosity was also recorded as ranging between 48.1% to 53.8%, with samples 1, 2, and 3 recordings at 49.4%, 48.1%, and 53.8% respectively (Table 3). The overall observation indicates that filter samples 1 and 2 had lower pore properties relative to filter sample 3. Table 3 shows the results from the MIP experiment.

Gas Physisorption Results

The results of the gas physisorption experiment on three randomly selected samples of the NHCWF filter candle were captured in isotherm profiles (Appendix E) and were further used for Brunauer Emmett and Teller (BET) analysis (Appendix F), and Barrett-Joyner-Halenda (BJH) mesopore analysis (Appendix G).

Gas physisorption isotherms of the three filter samples showed type II profiles, while two samples exhibited type H3 hysteresis according to the Brunauer-Deming-Deming-Teller (BDDT) methodology of classification (Thommes et al., 2015). The gas physisorption isotherms are shown in Appendix E. Table 4 also presents a summary of the results of all analyses performed on the results of the gas physisorption experiment. In Appendix E, it is observed that nitrogen is absorbed at varying degrees at low relative pressures. According to Thommes et al., this can be attributed to micropores (<20 Å diameter) and some mesopores. Adsorption at relative pressures below 0.05 P/Po indicates the presence of micropores (Thommes et al., 2015). The degree of adsorption however, corresponds to the micropore distribution within the sample. In Appendix Ea, Eb, and Ec the degree of nitrogen adsorption at relative pressures below 0.05 P/Po is recorded as approximately 0.06 cm^3/g, 7.50 cm^3/g, and 0.18 cm^3/g. This indicates that Appendix Eb which corresponds with filter 2 had the highest micropore distribution. Appendix Ea and Appendix Ec recorded much lower adsorption and hence may contain a relatively much lower micropore distribution. Again, the presence of micropores was verified for the three filters due to the appearance of positive intercepts in the isotherms. Table 4 shows the calculated values of the microporous parameters. These values were low, as expected. The micropore areas were much smaller than the external areas. Furthermore, micropore volumes accounted for filter 1 0.76%, filter 2 8.77% and filter 3 0.47%, respectively, of the total pore volume of each filter sample.

At around 0.60 P/Po, the isotherm begins to curve upwards in Appendix Eb. According to Thommes et al., this increase in adsorption around this region indicates the presence of meso-

Table 4. Summary of the results of the gas physisorption analysis of the NHCWF candles

Summary Report	Units	Sample 1	Sample 2	Sample 3
Surface Area				
Single point surface area at P/Po = 0.290540963	m^2/g	3.0568	35.308	1.9051
BET Surface Area	m^2/g	3.1690	36.002	2.3280
BJH Adsorption cumulative surface area (17.000–3,000.000 Å)	m^2/g	4.770	40.806	1.979
BJH Desorption cumulative surface area (17.000–3,000.000 Å)	m^2/g	7.6062	47.665	2.0513
Pore Volume				
Single point adsorption total pore volume (<2,140.957 Å at P/Po = 0.990892319)	cm^3/g	0.022489	0.103	0.004924
BJH Adsorption cumulative volume (17.000–3,000.000 Å)	cm^3/g	0.022061	0.101	0.004461
BJH Desorption cumulative volume (17.000–3,000.000 Å)	cm^3/g	0.022489	0.102	0.004426
Pore Size				
BJH Adsorption average pore diameter (4V/A)	Å	184.982	98.595	90.154
BJH Desorption average pore diameter (4V/A)	Å	118.269	85.629	86.306

pores (Thommes et al., 2015). This indicates the presence of mesopores in the samples. The final region of adsorption occurs at higher relative pressures and continues to increase as saturation is approached. This increase in adsorption volume is essentially asymptotic to the adsorption volume axis in all three graphs in Appendix E. According to Thommes et al., in nitrogen adsorption, macropores larger than about 3,000 Å in diameter are too large to be filled as saturation is approached which results in an asymptotic increase in adsorption volume (Thommes et al., 2015). This means the asymptotic nature of the adsorption isotherm to the adsorption volume axis of the three graphs in Appendix E may be due to the incomplete filling of pores (macropores) in the samples.

Except for the sample from Appendix Ec which showed no hysteresis, the samples of Appendix Ea and Appendix Eb showed the presence of hysteresis. The hysteresis loops of these isotherms are consistent with the type H3 hysteresis. This type of hysteresis is associated with type II isotherms and is observed as a plate-like layered structure (Thommes et al., 2015). The presence of hysteresis in Appendix Ea and Appendix Eb confirms the presence of open-ended pores distribution below approximately 3,000 Å in diameter. This is as a result of the variation in the adsorption and desorption mechanisms. Whilst adsorption takes place by capillary condensation of adsorbate, desorption takes place by evaporation of adsorbate. For an open-ended pore, these two processes take place at different relative pressures. Desorption takes place at a lower relative pressure, whilst adsorption takes place at a higher relative pressure. For close-ended pores, however, both adsorption and desorption take place at about the same relative pressures. The absence of hysteresis in Appendix Ec on the other hand indicates the absence of open-ended pores distribution below approximately 3,000 Å in diameter (Thommes et al., 2015).

In this study, all three BET isotherms had positive Y-intercepts and positive C values (100.918204, 100.918204, 9.201639 respectively). However, with the exception of filter 3, whose plots were not exactly linear and had a correlation coefficient less than 0.999 (0.9708660), filter 1 and filter 2 were linear over the relative pressure range from 0.05 to 0.3 and hence recorded a correlation coefficient greater than 0.999 (0.9991548 and 0.9996990 respectively). This means that whilst the BET analysis can give a true depiction of the specific surface area of filter 1 and filter 2 it may not give correct results if used for the specific surface area determination of filter 3 (Thommes et al., 2015; Zereffa and Desalegn, 2019). The BJH pore size distribution (PSD) was obtained by inverting both the adsorption and desorption branches of the isotherm for the filter candle samples. The parameter $\partial V/\partial \log(D)$ is used because the area under the curve between any two pore diameters can be used to assess the partial porosity for each pore diameter range. In a classical adsorption-desorption isotherm, the desorption isotherm is preferred over the adsorption isotherm in BJH analysis (Thommes et al., 2015). For filters 1 and 2, the distribution is unimodal with a major peak at 26 Å and between 65–75 Å respectively. Filter 3 on the other hand, has a multimodal distribution with a major peak between 100–120 Å and other minor but prominent peaks at ranges lower than the most prominent peak.

Fourier Transform Infrared (FTIR) Results

Figure 4a is the FTIR results of an unused NHCWF filter candle with an LRV of 3.86, whilst Figure 4b is the FTIR result of a 14-month used NHCWF candle with an LRV of 1.24 after processing about 700 gallons of untreated water. The FTIR spectrum of Figure 4a shows a peak at 3304 cm^{-1}, which corresponds with hydroxyl (OH) stretching vibrations, and the peaks at 2916 and 2848 and also corroborated by the peaks between 1470 and 720 cm^{-1}, correspond with the stretching and bending vibrations of a linear chain aliphatic compound. The absorbance at peaks between 1200–600, in both Figure 4a and Figure 4b, also corresponds to kaolinite (clay material such as Si-O-Ti, Si-O-Al, Mg/Al-OH).

Filtration Rate Results

Figure 5 shows that the flow (filtration) rate of the NHCWF filtering system generally decreased over the 130-minute dura-

Table 5. Log Reduction Values (LRV) for *Bacillus subtilis* and *Escherichia coli* of three samples of NHCWF filter samples

Experiment	Type	Sample 1	Sample 2	Sample 3	Mean ($\bar{x}$)	SD (s)
Pour Plating	*B. subtilis*	5.04	4.44	4.61	**4.70**	**±0.31**
	E. coli	5.42	4.61	5.63	**5.22**	**±0.54**
ATP Bioluminescence	*B. subtilis*	3.56	3.02	3.16	**3.25**	**±0.28**
	E. coli	3.42	2.97	3.09	**3.16**	**±0.23**
Optical Density	*B. subtilis*	4.03	3.95	3.78	**3.92**	**±0.13**
	E. coli	4.26	3.80	4.26	**4.11**	**±0.27**

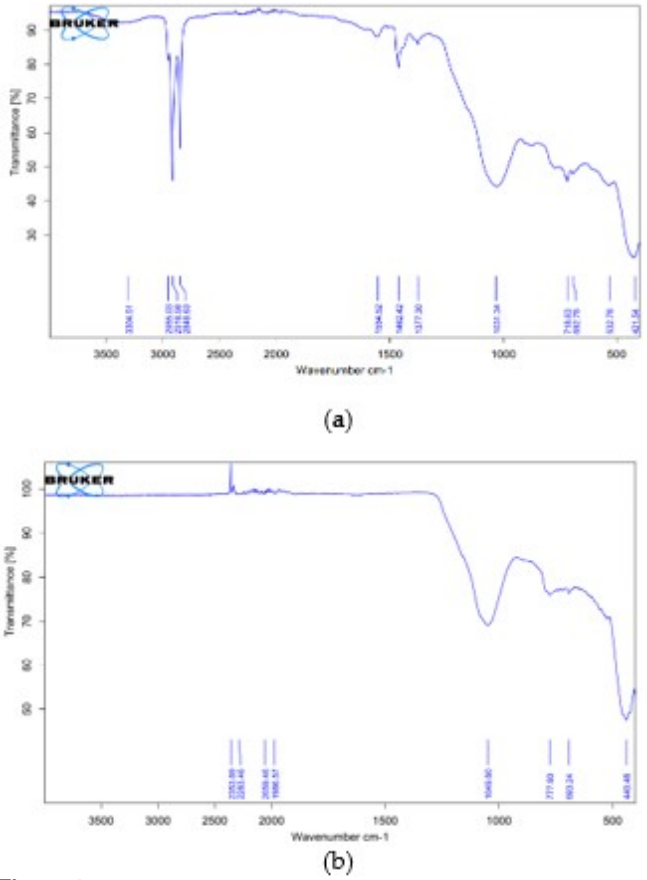

Figure 4. FTIR spectroscopy of NHCWF filter candles (a) unused filter candle

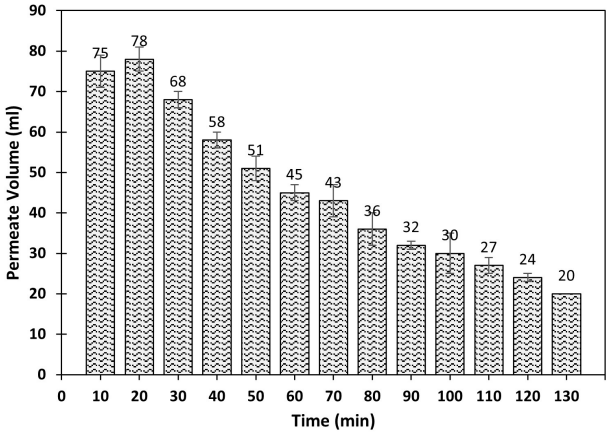

Figure 5. The flow rate of a sample filter at different time intervals for every 10 min

tion of the experiment. This observation is explained by Darcy flow, which applies to the relationship between the water sample and the ceramic membrane it permeates. It establishes that the flow velocity is directly proportional to the pressure gradient and inversely proportional to fluid viscosity (Elsevier, 2015).

This explains the generally decreasing filtration rate over the course of the experiment. As the filtration proceeds, the quantity of water in the receiver decreases with a concomitant increase in contaminants due to the retention abilities of the filter. This thereby results in a decrease in water pressure accompanied by an increase in its viscosity. The cumulative effect of these phenomena results in the gradual decrease in the permeate volume of water reaching the dispenser, hence the downward trend of the filtration rate.

The initial rise in the permeate volume from 75 ml to 78 ml, on the other hand, can be attributed to the phenomenon of imbibition by the filter. Whilst the first drop of water may have triggered the start of the timer, the matrix of the filter had to be fully submerged with water to record the real filtration rate of the filter for a given water level (height) (Obiri-Danso et al., 2003). The time it takes for the filter matrix to fully submerge in water reduces the initial amount of percolate water obtained and accounts for the initial bump in the percolate volume at the early stages of the experiment.

The average filtration rate of the NHCWF filter was obtained as 4.5 ± 0.3 mL min^{-1} or 270 mL h^{-1}.

Bacteria Retention Ability Results

The log reduction values (LRVs) of each of the three (3) NHCWF filter samples were calculated from the result of the pour plating experiment (Figure 6a), ATP bioluminescence experiment (Figure 6b), and optical density experiment (Figure 6c) conducted.

The results of these experiments showed variation in LRV across both the analytical method and filter samples used; however, the LRV values generally ranged between 3–5, depending on the analytical method used, as shown in Table 5.

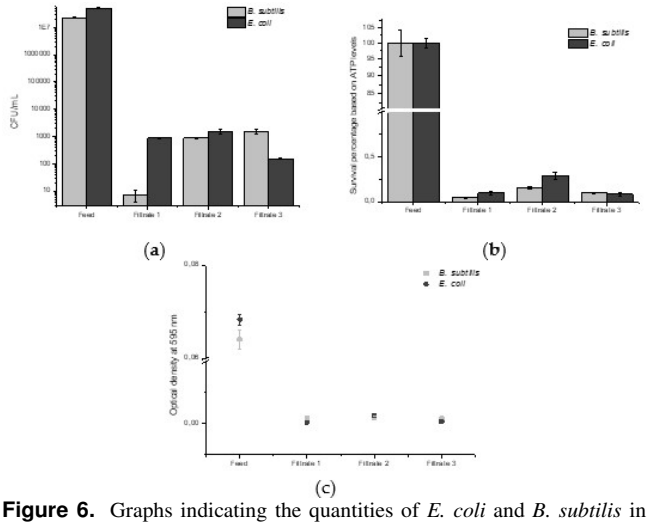

Figure 6. Graphs indicating the quantities of *E. coli* and *B. subtilis* in NHCWF-treated water samples before and after treatment using (a) pour plating experiment, (b) ATP bioluminescence assay

The wide variations in the LRV results can be attributed to the variations in what each of the experimental methods checks for, hence, resulting in differences in how they may be interpreted.

Whilst the pour plating method specifically estimates the number of viable *E. coli* and *B. subtilis* present in the water samples, the other methods may not be specific to these measurements. The ATP bioluminescence experiment measures metabolic activity, capturing both viable and viable but non-culturable (VBNC) bacteria, which can be important for assessing overall water quality. Optical density experiment, on the other hand, offered a quick estimate of the overall biomass based on turbidity.

The premise for the interpretation of these results, therefore, depends on the metric by which it is being evaluated. The results for the pour plating method may be used for bacteria-specific LRV comparison, whilst those of the ATP bioluminescence method may be ideal for a more generic LRV comparison. LRVs were calculated on a per-trial basis and averaged across replicates as shown in Table 5.

Statistical comparisons among the experimental methods and among the filter samples used for the experiment were conducted using one-way ANOVA, with significance defined at $p < 0.05$.

For the analysis of *B. subtilis* retention ability of the NHCWF filters, a one-way ANOVA analysis showed that there was a significant difference among the three experimental methods with respect to the LRV results obtained, $F(2, 6) = 24.88$, $p < .001$. Post hoc testing further revealed significant differences between all three methods. However, the same analysis showed no significant differences among the three filter samples used, $F(2, 6) = .275$, $p = .769$.

Similarly, for the analysis of *E. coli* retention ability of the NHCWF filters, a one-way ANOVA analysis showed that there was a significant difference among the three experimental methods with respect to the LRV results obtained, $F(2, 6) = 23.06$, $p = .002$. Post hoc testing further revealed significant differences between all three methods. However, the same analysis showed no significant differences among the three filter samples used, $F(2, 6) = .280$, $p = .765$.

These findings indicate that the experimental methods used may be measuring different variables and hence are not supplementary. On the other hand, the filter samples used are similar in their LRV values output for both *B. subtilis* and *E. coli*, hence indicating their ability to remove *B. subtilis* and *E. coli* from water to approximately the same extent.

Discussion

Potent Water Purification Alternative

The Nnsupa Household Ceramic Water Filter (NHCWF) represents an exceptional advancement in water purification, seamlessly integrating cutting-edge fabrication techniques such as advanced sintering processes and precision material engineering with a robust foundation in material science (UNICEF, 2020). Through rigorous performance assessments, the NHCWF emerges as a compelling alternative to existing ceramic filters. It excels in multiple domains: filtration efficiency, which ensures the effective removal of contaminants (Lantagne et al., 2010); flow rate optimization, which balances speed with thoroughness (Lantagne et al., 2010); structural durability, which guarantees long-term reliability under various conditions (Lantagne et al., 2010); and an extended operational lifespan that minimizes maintenance demands. This multi-faceted performance underscores the filter's suitability for diverse contexts and highlights its potential to address critical challenges in water purification with exceptional efficacy. These characteristics present the NHCWF as a potent option among household water filtration technologies in addressing critical challenges faced by residential users.

Comparison with Existing Technologies

The Nnsupa household ceramic water filter (NHCWF) was designed to provide a low-cost and less hazardous alternative to silver-embedded ceramic filters without compromising filtration efficiency and water quality. To this end, production material characteristics and availability, fabrication methods including sintering temperature, and filtration setup were the focal areas for innovation.

Designed as a bell-shaped filter candle, the NHCWF filter is shorter, slimmer, and has wider product variations than its commercially available household water treatment counterparts (Figure 7). It however possesses characteristics that make it a viable household water treatment solution.

The NHCWF showed favourable filter performance regarding its bacterial retention abilities as assessed using the bacterial log reduction value (LRV). The average LRV achieved was 5.2 for *E. coli* and 4.7 for *B. subtilis*, representing an approximation of a 99.999% reduction in both bacterial species (Valdiviezo Gonzales et al., 2021). Comparatively, commercial ceramic filters typically achieve an LRV of around 3.0–5.0 for similar tests with a few exceptions, as shown in Figure 8. It also exceeds commonly cited benchmarks as shown in Table 6.

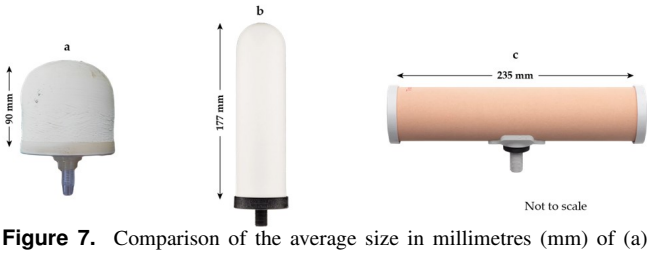

Figure 7. Comparison of the average size in millimetres (mm) of (a) NHCWF filter candle and other commercially available ceramic filters, including (b) Doulton Sterasyl and (c) Katadyn Rapidyn

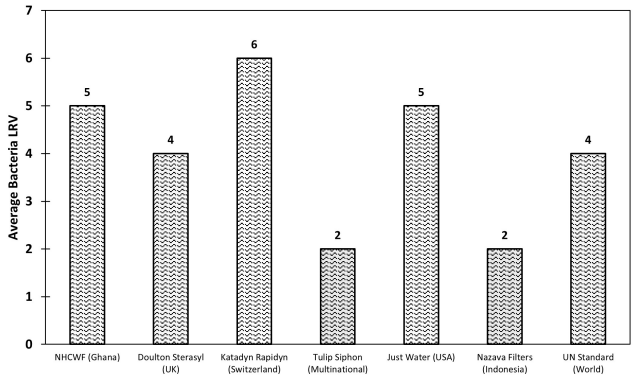

Figure 8. Figure 8. Comparison of average bacteria LRVs of NHCWF and other commercially available ceramic filters including Doulton Sterasyl, Katadyn Rapidyn, Tulip Siphon, Just Water, Nazava Filters, and the UN standard

This filtration performance can be linked to the presence of small and uniform pore size distribution and the presence of functional groups in the candle matrix, which enhances microbial filtration efficiency. The higher LRV is particularly important for use in regions with high contamination levels, as it ensures safer drinking water.

Whilst this novel filter demonstrates high microbial retention due to its fine pore structure, a key trade-off is its slow filtration rate (Valdiviezo Gonzales et al., 2021). It has a filtration rate of 270 mL h^{-1}, which is relatively lower than the UN household water filtration standard rate of at least 1700 mL h^{-1}, which allows water to be poured directly into a cup. This limitation is partly linked to the short and slim structure of the NHCWF filter relative to other commercially available filters that meet the UN's flow rate standard. Whilst the flow rate of the NHCWF system cannot effectively support the direct pouring of filtered water for consumption, it safely stores water in a dispenser, thereby indirectly allowing for the instantaneous pouring of filtered water without recontamination.

The NHCWF filter is also cost-effective. Its low material cost and reduced energy consumption due to reduced sintering temperature make it more cost-effective, such that its unit cost estimate is nine times ($1.37) less than the average unit cost of other commercially available ceramic filters ($12.85). These benefits translate into both competitive market prices and applicability in low-income areas.

Given NHCWF's high bacterial removal efficiency, low production cost, and mitigated flow rate limitation, the NHCWF filtering system is an attractive low-cost alternative to commercially available silver-embedded ceramic filters for household water treatment.

Mechanistic Insights

Microstructural Contributions to Optimal Performance

The NHCWF's exceptional performance is deeply rooted in its microstructural characteristics and precision fabrication. Scanning electron microscopy (SEM) analysis reveals a textured microstructure with interconnected pores that optimize mechanical strength and filtration efficiency (Li et al., 2016). Mercury intrusion porosimetry confirms a uniform pore diameter distribution ranging from 1 to 10 μm, with a median diameter (d_{50}) of 6.9 μm. This uniformity is pivotal for maximizing bacterial retention without compromising water permeability.

The interconnected pore network significantly enhances filtration efficacy. Gas physisorption experiments confirm that micropores ($\leq$20 Å) and mesopores ($\leq$65–75 Å) work in synergy to remove contaminants. Inferring from similar studies conducted by Maretto et al., the micropores are suspected to adsorb smaller molecules, ensuring precise retention of microscopic impurities (Maretto et al., 2014). Meanwhile, the mesopores, on the other hand, are suspected to enhance overall throughput by facilitating the transport and trapping of larger particles (Maretto et al., 2014). This complementary interaction optimizes filtration efficiency, distinguishing the NHCWF from other ceramic filters with less balanced pore size distributions. Cassava starch, used as a pore-forming agent, decomposes during sintering to create a uniformly porous structure. The precisely controlled sintering temperature of 1050 °C results in a dense yet permeable ceramic matrix, ensuring consistent performance across production batches.

Fabrication Methodology: Innovations in Material Science

The inclusion of kaolin and Mfensi clays not only bolsters mechanical properties but also improves material workability during production. The use of agricultural waste as a sintering fuel minimizes environmental impact while reducing production costs. Unlike traditional ceramic filters requiring sintering temperatures of up to 1200 °C, the NHCWF's lower sintering temperature conserves energy without sacrificing structural integrity.

BET surface area analysis underscores the critical role of material composition and sintering conditions in dictating the filter's overall performance characteristics. By analyzing specific surface areas and pore distributions, the study provides insight into how these factors influence adsorption efficiency and contaminant retention. For instance, higher surface areas achieved through precise control of sintering temperatures enhance the filter's ability to capture fine particulates and microorganisms, ensuring superior filtration outcomes. Specifically, although the surface area of the tested filters did not exceed 50 m^2 g^{-1}, the findings indicate that optimized

Table 6. Comparison with Guideline Benchmarks

Parameter	This Study	Guideline Benchmark	Source
Testing Condition	Wiwi River source	Standardized challenge water	WHO
Bacterial LRV	4.7 (*E. coli*)	≥4-log	WHO and UNICEF (2010)
Flow Rate	0.27 L h^{-1}	~1–2 L h^{-1} (typical household systems)	Tsaridou and Karabelas (2021); WHO and UNICEF (2010); World Health Organization (2018)

surface area still plays a crucial role in adsorption efficiency. The results suggest that even modest increases in surface area can significantly enhance microbial retention rates, providing valuable insights for tailoring surface properties to achieve specific performance goals in diverse filtration scenarios. Additionally, variations in pore geometry, influenced by material composition, play a pivotal role in optimizing water flow rates without compromising filtration precision. These findings not only highlight the technical sophistication of the NHCWF but also underscore its potential for scalability and adaptation across diverse operational environments.

Filters 1 and 2 demonstrate positive Y-intercepts and linear adsorption plots, indicative of efficient adsorption mechanisms and consistent pore accessibility. In contrast, Filter 3 exhibits a closed-pore configuration, which, while limiting overall adsorption capacity, suggests enhanced specificity for certain contaminants. This distinction in adsorption behavior highlights the tailored functionality of Filter 3, particularly in applications where selective adsorption is prioritized over general efficiency. These findings highlight the influence of fabrication parameters on performance consistency, addressing a common limitation in artisanal ceramic filters.

Potential Applications and Broader Impacts

Emergency and Disaster Response: Portability and Reliability

The lightweight and compact design of the NHCWF enhances its portability, making it a vital resource during natural disasters or emergency scenarios where access to clean water is disrupted. For example, in regions affected by severe flooding or hurricanes, where traditional water supply systems are often compromised, the NHCWF can be quickly deployed to provide a reliable source of potable water. Its ease of transportation and rapid setup make it particularly valuable for humanitarian organizations operating in these challenging environments, ensuring that affected communities have access to safe drinking water when they need it most. With a filtration rate of 0.27 L h^{-1} (270 mL h^{-1}), the NHCWF can meet the basic daily needs of a small household, providing a reliable source of potable water during emergencies. Its low production cost and minimal maintenance requirements further solidify its utility for humanitarian organizations operating in resource-limited settings.

Economic and Environmental Benefits

At a production cost of $1.37 per filter candle, the NHCWF is highly economical, particularly for low-resource settings as observed in multiple areas in developing countries. Its affordability arises from the use of locally sourced materials and energy-efficient manufacturing processes. In comparison, commercial ceramic filters often exceed $10 per unit, underscoring the NHCWF's cost advantage.

Environmentally, the use of agricultural waste as a sintering fuel significantly reduces carbon emissions and promotes sustainable practices. The filter's durability minimizes waste generation, as it retains structural integrity and filtration performance over a 14-month operational lifespan. This longevity reduces the frequency of replacements, amplifying its environmental benefits.

Broader Implications: Public Health and Economic Development

The widespread adoption of the NHCWF could profoundly impact public health and economic stability in developing regions. For instance, its deployment in rural areas lacking access to reliable water purification systems could lead to substantial reductions in waterborne diseases such as cholera and typhoid. Additionally, the low cost and long-term durability of the filter can alleviate financial burdens for families, freeing up resources for other necessities like education and healthcare. A case study in sub-Saharan Africa illustrates this potential, where similar initiatives have significantly improved community health metrics and economic resilience. By fostering self-reliance through localized production and job creation, the NHCWF could serve as a cornerstone for sustainable development in these areas. By providing an affordable and effective means of water purification, the filter has the potential to significantly reduce the prevalence of waterborne diseases, improving overall quality of life. Its long-term reliability decreases total ownership costs, fostering financial stability for households and communities.

Moreover, integrating the NHCWF into local economies could create new opportunities for employment and entrepreneurship. By leveraging local raw materials and production techniques, communities can establish self-sustaining supply chains, reducing dependence on imported alternatives and contributing to regional economic development.

Conclusions

This study successfully fabricated and characterized the Nnsupa non-chemical ceramic filter candle, demonstrating

its potential as an effective and affordable household water purification solution. The filter was developed using locally sourced kaolin clay, plastic clay, and cassava starch, eliminating the need for silver nanoparticles and thereby mitigating associated health and environmental risks. The Nnsupa filter was found to have a well-structured, porous microstructure that supports efficient microbial filtration. Its pore sizes range from 0.001 to 10.0 μm, ensuring effective contaminant removal. Notably, the filter exhibited bacterial log reduction values (LRVs) ranging between 4 (99.99%) and 5 (99.999%), meeting both Ghanaian and WHO drinking water standards. Additionally, its flow rate of 0.27 L h^{-1} augmented with a filtrate reservoir makes it suitable for household applications.

Key Takeaways

The microstructural analysis using scanning electron microscopy (SEM) confirmed a closely packed ceramic matrix with scattered porosity, ensuring mechanical stability and consistent filtration performance. Mercury intrusion porosimetry and nitrogen gas physisorption analysis confirmed the presence of micropores, mesopores, and macropores, which contribute to the filter's high contaminant retention capabilities. Fourier transform infrared (FTIR) analysis further indicated the presence of functional groups that are actively involved in water filtration processes and degrade over time with use. The cost analysis demonstrated the economic viability of the filter, with a production cost of approximately $1.37 per unit, making it an affordable alternative to commercially available silver-embedded filters.

Future Research

While the Nnsupa ceramic filter has shown significant promise in providing clean drinking water, several areas warrant further research and optimization. Future studies should focus on improving the flow rate without compromising filtration efficiency. This may involve optimizing the material composition and sintering temperature to achieve a balance between porosity and mechanical strength. Additionally, long-term performance studies should be conducted to evaluate the durability of the filter over extended periods of use, particularly in varying environmental conditions.

Also, research into the theoretical flow models of NHCWF candles—including the rheology of casting materials for the fabrication of the filter candle—should be conducted to improve the quality of the models with further refinement, including manufacturing and product variable terms to meet diverse water treatment needs. The relationship between particle size distribution and pore morphology of NHCWF candles should also be studied to help use particle size as a means of improving the filtration quality of the NHCWF candle. Investigating the effects of changes in feed water volume on the flow rate dynamics of the NHCWF candle. Investigating the causal relationship between the consumption of functional groups lining the matrix and the bacteria retention capacity (LRV) of the NHCWF candles.

Another promising avenue for future research is the exploration of alternative natural additives to enhance the filter's antimicrobial properties. Investigating plant-based biocides, metal oxide nanoparticles, or functionalized ceramic coatings could further improve bacterial reduction efficiency while maintaining the filter's non-chemical approach. Additionally, studies on the impact of prolonged usage on filter performance, such as potential clogging and regeneration techniques, would be beneficial for increasing the filter's lifespan and cost-effectiveness.

Final Thoughts

In conclusion, the Nnsupa non-chemical ceramic filter candle presents a sustainable, low-cost, and efficient water purification solution, addressing critical water safety challenges in low-resource communities. Its ability to remove bacteria effectively, coupled with its affordability and ease of fabrication, makes it a viable alternative to conventional silver-embedded ceramic filters. With continued research and development, the Nnsupa filter has the potential to significantly contribute to achieving global clean water access goals, particularly in underserved regions. By refining its design, scaling production, and exploring innovative material enhancements, this technology can play a pivotal role in ensuring safe and affordable drinking water for all.

Author Contributions

Michael Commeh: Conceptualization, Writing - Original draft preparation, Data curating, Project administration, Investigation, Validating, Formal analysis and funding.
James Hawkins Ephraim: Writing – Review and Editing, Supervision, and Validation.
Kwabena Bonsu Kusi: Writing - Original draft preparation, Formal analysis, methodology, validation.
David Dodoo-Arhin: Data curating, Writing – Review and Editing, validation.

Declaration of Competing Interest

The authors declare no competing interest.

Data Availability Statement

The data that support the findings of this study are available from the corresponding author (Michael Commeh) upon reasonable request.

Acknowledgments

I would like to thank the Department of Theoretical Biological Science, KNUST, Water and Sanitation Laboratory of Civil Engineering Laboratory, KNUST, and Regional Water and Environmental Sanitation Centre Kumasi (RWESCK) of Kwame Nkrumah University of Science and Technology, Ghana for supporting the project. My ultimate thanks go to God, who has been present with me through the work and made the work a success. His name be glorified.

Appendix A: A schematic representation of the NHCWF filter production process

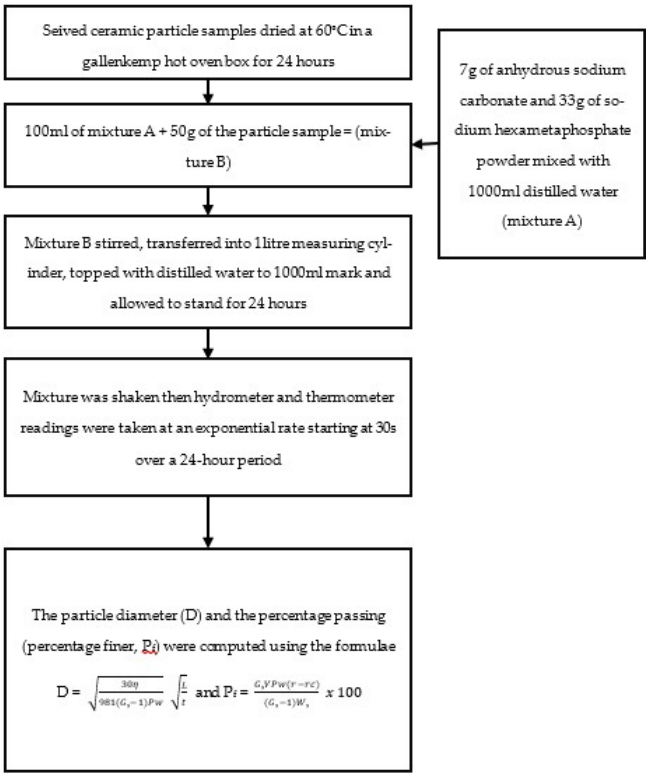

Appendix B: Particle size distribution analysis process

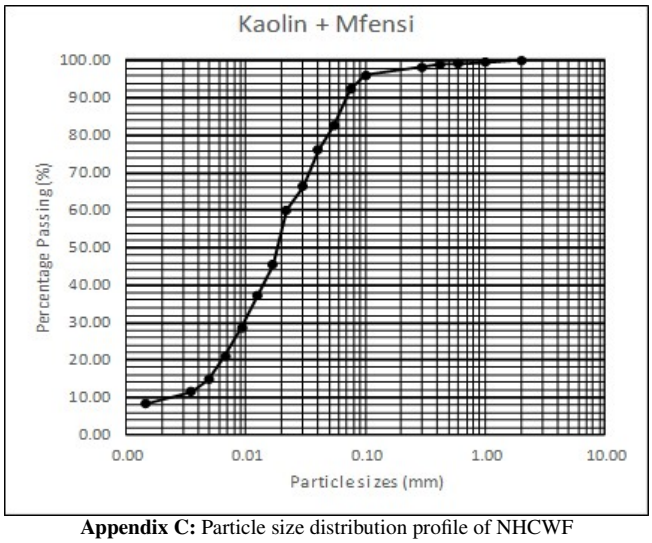

Appendix C: Particle size distribution profile of NHCWF

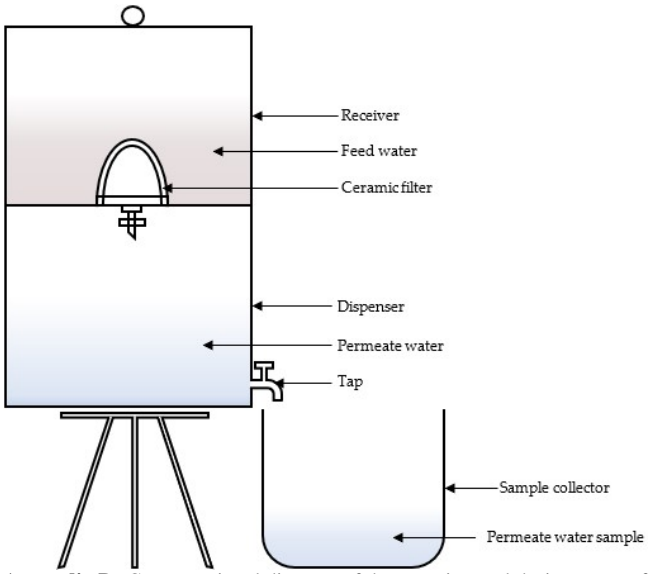

Appendix D: Cross-sectional diagram of the experimental design setup of the NHCWF filtering process

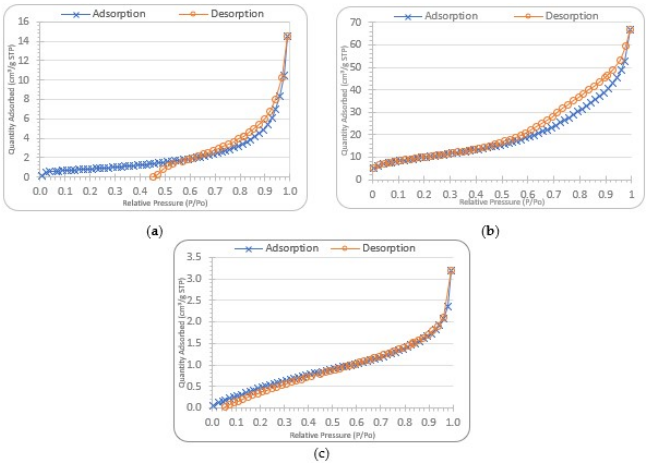

Appendix E: Nitrogen gas physisorption isotherms for NHCWF filter samples

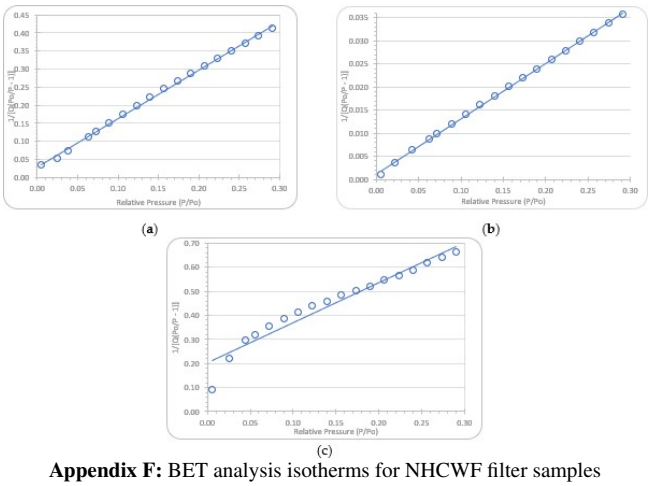

Appendix F: BET analysis isotherms for NHCWF filter samples

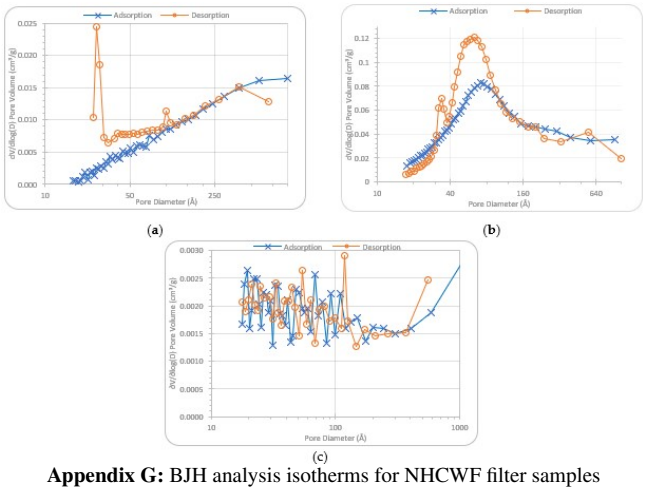

Appendix G: BJH analysis isotherms for NHCWF filter samples

References

Aakumiah, P. O. (2007). Water Management and Health in Ghana: Case Study - Kumasi. Master's thesis, Linköping universitet. https://urn.kb.se/resolve?urn=urn:nbn:se:liu:diva-15239.

Campbell, J. (2010). High-Throughput Assessment of Bacterial Growth Inhibition by Optical Density Measurements. *Current Protocols in Chemical Biology*, 2(3):195–208. https://doi.org/10.1002/9780470559277.ch100115.

Deininger, R. A. and Lee, J. (2001). Rapid determination of bacteria in drinking water using an ATP assay. *Field Analytical Chemistry & Technology*, 5(4):185–189. https://doi.org/10.1002/fact.1020.

Ehdaie, B., Rento, C. T., Son, V., Turner, S. S., Samie, A., Dillingham, R. A., and Smith, J. A. (2017). Evaluation of a Silver-Embedded Ceramic Tablet as a Primary and Secondary Point-of-Use Water Purification Technology in Limpopo Province, S. Africa. *PLOS ONE*, 12(1):e0169502. https://doi.org/10.1371/journal.pone.0169502.

Elsevier (2015). *Fundamentals of fluid flow through porous media*. Elsevier. https://doi.org/10.1016/B978-0-12-800219-3.00009-7.

in D. Team, O. and Roser, M. (2023). Ensure access to water and sanitation for all. https://ourworldindata.org/sdgs/clean-water-sanitation.

Kakulu, R. K. (2012). Diarrhoea among under five Children and Household Water Treatment and Safe Storage Factors in Mkuranga District, Tanzania. Master's thesis, Muhimbili University of Health and Allied Sciences. https://core.ac.uk/display/11307835.

Lantagne, D., Klarman, M., Mayer, A., Preston, K., Napotnik, J., and Jellison, K. (2010). Effect of production variables on microbiological removal in locally-produced ceramic filters for household water treatment. *International Journal of Environmental Health Research*, 20(3):171–187. https://doi.org/10.1080/09603120903440665.

Li, L., Chen, M., Dong, Y., Dong, X., Cerneaux, S., Hampshire, S., Cao, J., Zhu, L., Zhu, Z., and Liu, J. (2016). A low-cost alumina-mullite composite hollow fiber ceramic membrane fabricated via phase-inversion and sintering method. *Journal of the European Ceramic Society*, 36(8):2057–2066. https://doi.org/10.1016/j.jeurceramsoc.2016.02.020.

Lyon-Marion, B. A., Mittelman, A. M., Rayner, J., Lantagne, D. S., and Pennell, K. D. (2018). Impact of chlorination on silver elution from ceramic water filters. *Water Research*, 142:471–479. https://doi.org/10.1016/j.watres.2018.06.008.

Maretto, M., Blanchi, F., Vignola, R., Canepari, S., Baric, M., Iazzoni, R., Tagliabue, M., and Papini, M. P. (2014). Microporous and mesoporous materials for the treatment of wastewater produced by petrochemical activities. *Journal of Cleaner Production*, 77:22–34. https://doi.org/10.1016/j.jclepro.2013.12.070.

Medici, S., Peana, M., Nurchi, V. M., and Zoroddu, M. A. (2019). Medical Uses of Silver: History, Myths, and Scientific Evidence. *Journal of Medicinal Chemistry*, 62(13):5923–5943. https://doi.org/10.1021/acs.jmedchem.8b01439.

Meyers, A., Furtmann, C., and Jose, J. (2018). Direct optical density determination of bacterial cultures in microplates for high-throughput screening applications. *Enzyme and Microbial Technology*, 118:1–5. https://doi.org/10.1016/j.enzmictec.2018.06.016.

Micromeritics (2013). 3Flex - Sample Preparation for Physisorption Analyses. Micromeritics. https://www.micromeritics.com/3flex-sample-preparation-for-physisorption-analyses/.

Mikelonis, A. M., Lawler, D. F., and Passalacqua, P. (2016). Multilevel modeling of retention and disinfection efficacy of silver nanoparticles on ceramic water filters. *Science of The Total Environment*, 566–567:368–377. https://doi.org/10.1016/j.scitotenv.2016.05.076.

Mittelman, A. M., Lantagne, D. S., Rayner, J., and Pennell, K. D. (2015). Silver Dissolution and Release from Ceramic Water Filters. *Environmental Science & Technology*, 49(14):8515–8522. https://doi.org/10.1021/acs.est.5b01428.

Null, C., Stewart, C. P., Pickering, A. J., Dentz, H. N., Arnold, B. F., Arnold, C. D., Benjamin-Chung, J., Clasen, T., Dewey, K. G., Fernald, L. C. H., Hubbard, A. E., Kariger, P., Lin, A., Luby, S. P., Mertens, A., Njenga, S. M., Nyambane, G., Ram, P. K., and Colford, J. M. (2018). Effects of water quality, sanitation, handwashing, and nutritional interventions on diarrhoea and child growth in rural Kenya: a cluster-randomised controlled trial. *The Lancet Global Health*, 6(3):e316–e329. https://doi.org/10.1016/S2214-109X(18)30005-6.

Nunnelley, K., Smith, J. A., Smith, M. Y., and Samie, A. (2016). A New Method for Nanosilver Application in Ceramic Water Filters. In *World Environmental and Water Resources Congress 2016*, pages 292–298. ASCE. https://doi.org/10.1061/9780784479865.031.

Obiri-Danso, K., Okore-Hanson, A., and Jones, K. (2003). The microbiological quality of drinking water sold on the streets in Kumasi, Ghana. *Letters in Applied Microbiology*, 37(4):334–339. https://doi.org/10.1046/j.1472-765X.2003.01403.x.

Oyanedel-Craver, V. A. and Smith, J. A. (2008). Sustainable Colloidal-Silver-Impregnated Ceramic Filter for Point-of-Use Water Treatment. *Environmental Science & Technology*, 42(3):927–933. https://doi.org/10.1021/es071268u.

Ren, D. and Smith, J. A. (2013). Retention and Transport of Silver Nanoparticles in a Ceramic Porous Medium Used for Point-of-Use Water Treatment. *Environmental Science & Technology*, 47(8):3825–3832. https://doi.org/10.1021/es4000752.

Solomon, P. R. and Carangelo, R. M. (1982). FTIR analaysis of coal. 1. techniques and determination of hydroxyl concentrations. *Fuel*, 61(7):663–669. https://doi.org/10.1016/0016-2361(82)90014-X.

Thommes, M., Kaneko, K., Neimark, A. V., Olivier, J. P., Rodriguez-Reinoso, F., Rouquerol, J., and Sing, K. S. W. (2015). Physisorption of gases, with special reference to the evaluation of surface area and pore size distribution (IUPAC Technical Report). *Pure and Applied Chemistry*, 87(9-10):1051–1069. https://doi.org/10.1515/pac-2014-1117.

Tsaridou, C. and Karabelas, A. J. (2021). Drinking Water Standards and Their Implementation—A Critical Assessment. *Water*, 13(20):2918. https://doi.org/10.3390/w13202918.

UNICEF (2020). Household Water Treatment Filters - Product Guide. Technical report, UNICEF. https://www.hwts.info/products-technologies/a48a2cee/ceramic-candle-filter/technical-information.

United Nations (2023). Water and Sanitation. https://www.un.org/sustainabledevelopment/water-and-sanitation/.

Valdiviezo Gonzales, L. G., García Ávila, F. F., Cabello Torres, R. J., Castañeda Olivera, C. A., and Alfaro Paredes, E. A. (2021). Scientometric study of drinking water treatments technologies: Present and future challenges. *Cogent Engineering*, 8(1):1929046. https://doi.org/10.1080/23311916.2021.1929046.

Venis, R. A. and Basu, O. D. (2021). Mechanisms and efficacy of disinfection in ceramic water filters: A critical review. *Critical Reviews in Environmental Science and Technology*, 51(24):2934–2974. https://doi.org/10.1080/10643389.2020.1806685.

Wadhera, A. and Fung, M. (2005). Systemic argyria associated with ingestion of colloidal silver. *Dermatology Online Journal*, 11(1):12. https://doi.org/10.5070/D30832g6d3.

WHO and UNICEF (2010). *Progress on sanitation and drinking-water: 2010 update*. World Health Organization, Geneva. https://apps.who.int/iris/handle/10665/44272.

World Health Organization (2018). *A global overview of national regulations and standards for drinking-water quality*. World Health Organization, Geneva. https://apps.who.int/iris/handle/10665/272345.

Yang, H., Xu, S., Chitwood, D. E., and Wang, Y. (2020). Ceramic water filter for point-of-use water treatment in developing countries: Principles, challenges and opportunities. *Frontiers of Environmental Science & Engineering*, 14:79. https://doi.org/10.1007/s11783-020-1254-9.

Zagonel, G. F., Peralta-Zamora, P., and Ramos, L. P. (2004). Multivariate monitoring of soybean oil ethanolysis by FTIR. *Talanta*, 63(4):1021–1025. https://doi.org/10.1016/j.talanta.2004.01.008.

Zeng, Q., Chen, S., Yang, P., Peng, Y., Wang, J., Zhou, C., Wang, Z., and Yan, D. (2020). Reassessment of mercury intrusion porosimetry for characterizing the pore structure of cement-based porous materials by monitoring the mercury entrapments with X-ray computed tomography. *Cement and Concrete Composites*, 113:103726. https://doi.org/10.1016/j.cemconcomp.2020.103726.

Zereffa, E. A. and Desalegn, T. (2019). Preparation and characterization of sintered clay ceramic membranes water filters. *Open Material Sciences*, 5:24–33. https://doi.org/10.1515/oms-2019-0005.